PHYSICAL REVIEW B, VOLUME 64, 161403(R)

Mobility and bonding transition of C_{60} on Pd(110)

J. Weckesser,[1,2] J. V. Barth[1,*] and K. Kern[1,2]
[1]*Institut de Physique Expérimentale, Ecole Polytechnique Fédérale de Lausanne, CH-1015 Lausanne, Switzerland*
[2]*Max-Planck-Institut für Festkörperforschung, Heisenbergstraße 1, D-70569 Stuttgart, Germany*
(Received 9 May 2001; revised manuscript received 3 July 2001; published 28 September 2001)

Mobility and bonding of C_{60} on a Pd(110) surface were characterized by variable temperature scanning tunneling microscopy. Following adsorption at intermediate temperatures (435–485 K) the motion of single molecules could be directly monitored, and the corresponding tracer diffusion barrier was determined to be (1.4 ± 0.2) eV. Upon annealing to $\approx$700 K the molecules undergo an irreversible bonding transition resulting in a second, more strongly bound C_{60} species with different imaging characteristics. This is attributed to a local surface reconstruction where C_{60} sinks into the formed microscopic pits. The findings demonstrate that substrate restructuring may account for the coexistence of distinct C_{60} species at surfaces.

DOI: 10.1103/PhysRevB.64.161403 PACS number(s): 68.43.Jk, 68.37.Ef, 61.48.+c

The interaction between C_{60} and surfaces has attracted much interest in recent years, which is motivated by two aspects. First, from a technological point of view, the substrate-induced modification of the electronic and structural properties of C_{60} is an important question to be addressed for possible future applications in molecular electronics.[1–3] Second, from a fundamental point of view, the variety of both bond strength and bond character observed in the interaction between C_{60} and a substrate, ranging from weak van der Waals type[4–6] to strong chemisorption,[7] is exceptional and still far from being completely understood. In particular, the growth of C_{60} on a multitude of different metal surfaces was studied intensively,[8–16] as recently reviewed.[17,18] On most surfaces C_{60} tends to form well-ordered quasihexagonal close-packed overlayers with a nearest-neighbor separation close to that of the van der Waals bonded C_{60} solid. However, on some substrates two different C_{60} species were resolved by scanning tunneling microscopy (STM).[18–20] However, the origin for their different appearance is currently under controversial discussion and supposed to be either an electronic effect due to different orientations of the C_{60} cages or geometrically due to a C_{60} induced surface reconstruction. Even for the most extensively studied system, i.e., C_{60} on Ag(001), this issue could not be resolved unambiguously.[20,21] Strong substrate restructuring has been found, e.g., for C_{60} on Ni(110) (Ref. 10) and Au(110).[15]

Despite the large number of studies on the adsorption and growth there is no detailed investigation of C_{60} surface diffusion. The thermal motion plays a crucial role in the film growth and an accurate knowledge is indispensable to fully understand the ordering and interactions at surfaces. Here we report the first direct investigation, to the best of our knowledge, of C_{60} diffusion and aggregation at a metal surface at the single molecule level. We employed variable temperature STM, which has proven to be a powerful tool for the direct investigation of surface diffusion and binding characteristics of adsorbed complex molecules at metal surfaces.[22–24] A rather large energy barrier $[(1.4\pm0.2)\ \mathrm{eV}]$ and attempt frequency $(10^{14.4\pm0.4}\ \mathrm{s}^{-1})$ for the tracer diffusion is determined. Our results furthermore reveal that C_{60} molecules sink into the substrate resulting in a much higher C_{60}-Pd coordination upon thermal annealing.

The experiments were performed with a home-built variable temperature STM operational in the temperature range 40–800 K, incorporated in a standard ultrahigh vacuum (UHV) chamber with a base pressure of $\approx 2\times10^{-10}$ mbar. The Pd(110) crystal was prepared by cycles of argon ion sputtering (700 eV, 4 μA/cm^2) and subsequent annealing (1000 K) resulting in large defect-free terraces of typically 1000 Å width, C_{60} was deposited by a conventional Knudsen-cell at background pressures of $\approx 5\times10^{-10}$ mbar. The employed deposition rate was $\approx 1\times10^{-4}$ ML/s as calibrated by STM data [1 ML corresponds to one adsorbed molecule per Pd surface atom, the dense-packed phase (physical ML) amounts to 0.12 ML (Ref. 25)].

In Fig. 1 the thermal motion of C_{60} molecules and Pd substrate atoms is visualized. The two STM images shown have been taken at the same surface area (time lapse $\approx$1600 s) with the substrate temperature held at 437 K. They were selected from a series of images with a respective time lapse of $\approx$100 s. The arrows marked with (m) show isolated C_{60} molecules on a flat terrace the positions of which have changed. The temperature dependence of the molecular displacements has been used to determine the respective hopping rates and the energy barrier for diffusion of isolated C_{60}. The hopping rate ν at a specific temperature was obtained by determining the fraction of isolated molecules that did not move in a certain time interval τ (typically given by the number of scanlines required to image C_{60} entirely) in an ensemble (e.g., the entire number of single molecules in an image). Since the probability that the adsorbate remains immobile is given by $P=\exp[-\nu\tau]$, the corresponding hopping rates, i.e., those for tracer diffusion, can be extracted easily from a statistical data analysis cf. Refs. 22, 23, and 26. Due to the anisotropy of the Pd(110) surface, where the $[1\bar{1}0]$ direction is oriented along close-packed Pd atomic rows [cf. inset Fig. 1(a)] the diffusion barrier along $[1\bar{1}0]$ is expected to be smaller than along [001]. Indeed a close inspection of the STM data shows that motions along the $[1\bar{1}0]$ direction are predominant and the hopping rate determination was performed assuming one-dimensional motions. Nevertheless, very rarely displacements in the perpendicular [001] cannot be excluded. They are statistically insignificant. Thus the

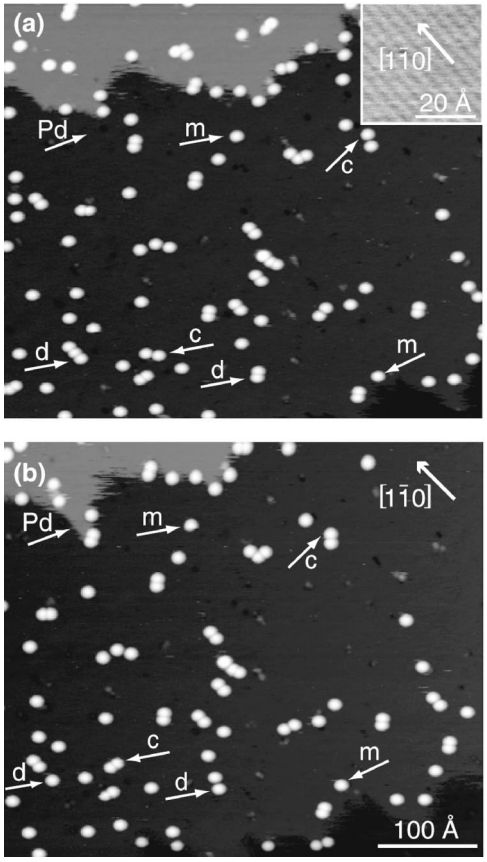

FIG. 1. Series of STM images monitoring thermal motions of metastable C_{60} molecules on Pd(110) at $T=437$ K. The time lapse between the two selected images from a data series monitoring the same surface area is 1600 s. Arrows indicate: (*m*) single C_{60} monomers whose positions changed, (*c*) C_{60} cluster formation and (*d*) C_{60} cluster dissociation due to moving C_{60} molecules. The arrow in the top left corner of the STM image marked with (Pd) indicates the thermal motion of a monatomic substrate step. Note that two C_{60} molecules adsorbed on the lower step edge in (a) are embedded by the moving Pd terrace in (b) but are still bound to the lower terrace. In the inset of (a) a STM image with resolved close-packed Pd atom rows along the $[1\bar{1}0]$ direction of the anisotropic Pd(110) surface is represented.

mobility could not be reduced strictly to one dimension, as for diffusion of metal adatoms[27] or smaller molecules on the same surface.[22] This behavior is associated with the ball-shape of the C_{60} molecule interacting at each moment with an extended part of the substrates potential energy surface. The arrows marked with (*c*) and (*d*) show C_{60} cluster formation and dissociation, respectively. The fact that the formation and dissociation of C_{60} clusters readily takes place at 437 K signals weak lateral C_{60}-C_{60} interactions, which are presumably of the van der Waals type, as in the C_{60} bulk. This is in accordance with the desorption of the multilayer C_{60} at 455 K.[28] In contrast to integral methods the local information of STM offers the advantage to distinguish between these different processes and allows us to gain insight into diffusion of an isolated molecule on a flat terrace.

Diffusion rates could be successfully determined in the temperature interval 435–485 K with the instrumental and

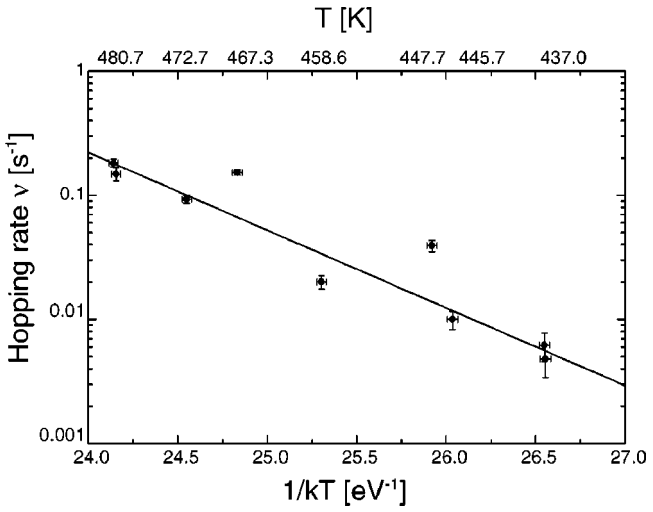

FIG. 2. Arrhenius plot of single molecule diffusion rates in the temperature interval between 435 and 485 K. The linear fit gives an energy barrier for C_{60} tracer diffusion of (1.4 ± 0.2) eV and an attempt frequency of $10^{14.4\pm0.4}\,s^{-1}$.

data analysis means at hand. With higher (lower) temperatures the limits in the scanning frequency (the small hopping rates) prevent from a sound data analysis. The STM data have been obtained in the constant current mode. It was impossible to manipulate the adsorbed molecules under any tunneling conditions, which reflects strong adsorbate-substrate interactions. The diffusion measurements were carried out with typical tunneling voltages of 1.2 V and currents below 0.5 nA, i.e., in the high tunneling resistance regime (>2 GΩ). We also investigated the possibility of tip-induced changes in the surface diffusitivity by performing measurements with different scanning frequencies and image sizes. However, no modifications in the diffusion characteristics were observed at the employed high tunneling resistances. The statistical hopping rate analysis is plotted in an Arrhenius representation in Fig. 2. For each temperature between 250 and 800 events have been counted. The linear fit yields an energy barrier associated with tracer diffusion along the close-packed direction of (1.4 ± 0.2) eV and a corresponding attempt frequency of $10^{14.4\pm0.4}\,s^{-1}$. The rather large value for the diffusion barrier signals strong interactions and directional bonding between the C_{60} carbon ring systems and the Pd surface atoms.

It is interesting to compare these results with the behavior of another large organic molecule investigated on the Pd(110) surface, i.e., 4-[*trans*-2-(pyrid-4-yl-vinyl)]benzoic acid (PVBA). With this species strong π bonding of the two ring systems to Pd surface atoms enforces a flat adsorption geometry.[29] The surface diffusion of PVBA is found to be strictly one-dimensional along the close-packed Pd troughs with an energy barrier of (0.83 ± 0.03) eV,[22] significantly inferior to that of C_{60}. The stronger adsorbate-substrate interactions for C_{60} than for PVBA indicate that not only the carbon atoms of C_{60} closest to the surface are involved in the bonding. Rather, even more distant C atoms are implied in the formation of the surface chemical bond. The attempt frequency for the PVBA/Pd(110) system amounts to

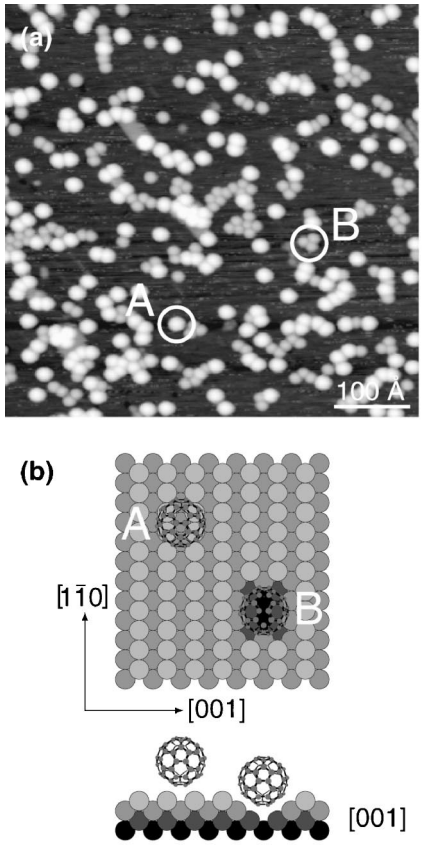

FIG. 3. (a) Pd(110) surface after evaporation of C_{60} at room temperature (0.06 physical ML) followed by annealing to ≈700 K and subsequent C_{60} evaporation at room temperature (0.03 physical ML). Two different molecular species are clearly discernible: the bright molecules [marked *A*: (5.5±0.2) Å high] are metastable and convert into the dark species [marked *B*: (3.1±0.2) Å high] upon annealing. (b) Model for the bonding configurations of metastable and stable C_{60}. Whereas the metastable C_{60} molecules (*A*) are bound on top of the unreconstructed Pd(110) surface, the stable C_{60} species (*B*) are accommodated in microscopic pits formed by the release of 8 Pd substrate atoms. The side view demonstrates the increased C-Pd coordination in the stable bonding configuration.

$10^{10.3\pm0.4}\,s^{-1}$ much lower than for C_{60}. In contrast to C_{60} the lateral interactions between PVBA and Pd are negligible. In the case of C_{60} the ball shape of the molecular geometry provides the additional possibility of lateral π bonding to Pd. This might also strongly modify the mechanisms involved in the thermal motion of C_{60} compared to that of atoms or simple molecules, which can be rationalized as a hopping between adjacent bonding sites. Due to the shape and size C_{60} can be a rolling buckyball, where high C-Pd coordination is retained, similar to theoretically suggested rolling motions of nickel clusters on a Au(110) surface.[30] The persistent lateral π bonding might energetically favor this process [cf. Fig. 3(b)]. The large prefactor could indeed be indicative of such a process. A rolling motion will likely be characterized by a rather flat potential energy surface close to the transition state which can produce a high prefactor.[31] A two-dimensional rotation scenario has been suggested to be responsible for the high prefactors seen in the diffusion of Ir_{19} clusters on Ir(111).

Another notable process visualized in the two STM images of Fig. 1 is the moving Pd substrate step in the upper left corner (marked by Pd). Two C_{60} molecules adsorbed on the lower step edge in (a) are embedded by moving Pd atoms in (b). From the height of the C_{60} molecules it is concluded that they are still bound to the lower Pd terrace surface layer. While stochastic step fluctuations typically occur at metal surfaces at sufficiently high thermal energies, the lateral attachment or pinning of Pd steps by C_{60} molecules was found to be characteristic with the present system. It indicates significant *lateral* attractive interactions between Pd atoms and C_{60} molecules. Due to the increased molecular coordination to Pd surface atoms, C_{60} is expected to be more strongly bound in this configuration. Cuberes *et al.*[12] reported C_{60} molecules on Cu(111) which have been trapped in nanometer-sized Cu vacancies after manipulating C_{60} over a step edge with a STM tip. They have still been bound to the second Cu layer below the surface.

At higher temperatures the mobility of C_{60} molecules does not increase continuously, rather their bonding characteristics change entirely. Upon annealing C_{60} molecules deposited at room temperature to ≈700 K (typically for a one minute period), the apparent height in the STM images decreases substantially. This is most conspicuous in the following experiment: A small amount of C_{60} (0.06 physical ML) is evaporated on a Pd(110) surface kept at room temperature. All C_{60} molecules are identically imaged and the height is determined to be (5.5±0.2) Å, slightly smaller than the hard sphere diameter of C_{60} (7.1 Å) reflecting the different electronic structure of C_{60} and the Pd surface. Upon annealing to ≈700 K, STM images taken at room temperature show again identical C_{60} molecules which are now more often found in clusters and the height has decreased to (3.1±0.2) Å. In the STM image shown in Fig. 3(a) an additional small amount of C_{60} (0.03 physical ML) has been evaporated with the sample held at room temperature. Two different molecular species are clearly discernible. The bright molecules are mostly isolated at the surface whereas the majority of the dark species is found in clusters. Complementary x-ray photoelectron diffraction measurements reveal that the C_{60} molecules remain unaffected for annealing up to ~1000 K and do not undergo any structural changes.[25] It is thus concluded that the bright molecules are metastable and convert into the dark species upon annealing. The single molecules within a C_{60} cluster can be easily distinguished. The apparent molecular shape in the STM images is deformed and clusters are imagedlike soap bubbles. This is not associated with a deformation of the C_{60} cage but rather reflecting the extension of electronic states which mediate the tunneling current. The intermolecular distance within a C_{60} cluster is with about 12 Å quite large and the strong perturbation of electron density is surprising for the expected van der Waals interactions. The mobility of the dark species is much lower which reflects a stronger adsorbate-substrate interaction. Determination of the energy barrier for diffusion of the dark species was impossible in view of the clustering and instrumental limita-

tions. These results demonstrate that the transition is thermally activated, but the detailed nature of the bonding change is still unclear. No dependency of the apparent C_{60} molecular height and the bias voltage between -5 V and $+5$ V is found. The height difference between metastable and stable C_{60} amounts to 2.4 Å independent of the tunneling conditions. This value is close to twice a monatomic step (1.38 Å) on the Pd(110) surface. It is thus suggested that Pd atoms are released and the C_{60} molecules sink into the Pd substrate in order to increase C_{60}-Pd coordination leading to stronger lateral interactions. This is supported by the strong lateral C_{60}-Pd interactions inferred from the analysis of Fig. 1. Due to the high mobility of Pd adatoms at elevated temperature ($\approx$700 K) the released substrate atoms attach at step edges.

A model for the two bonding configurations is represented in Fig. 3(b): The metastable C_{60} species is bound on top of the unreconstructed Pd(110)(1×1) surface. Upon thermal activation, the stable C_{60} species is accommodated in a vacancy formed by eight Pd atoms released out of the first two layers, following ideas for the substrate atomic arrangement with C_{60} in microscopic pits at Au(110).[15] High temperatures are necessary to break the Pd-Pd bonds; the corresponding energy cost is overbalanced by the gain in energy due to the newly formed C-Pd bonds. Several possible reasons exist for the small discrepancy between the expected geometric and the measured height difference: it can be related to the higher C-Pd coordination in the relaxed bonding configuration changing the electronic structure, to a relaxation of the substrate or to tip convolution effects. The side view demonstrates the increased C_{60}-Pd coordination in the stable bonding configuration. STM measurements performed with regular superstructures evolving upon annealing higher coverages[25] reveal that a further species with an intermediate STM imaging height exists and underline that the pits must be two layers deep.

We are not aware of other organic adsorbates inducing a reconstruction of the Pd(110) surface. However, a similar local reconstruction has been reported recently for the C_{60}/Au(110) system, for potassium on Cu(110) (Ref. 32) or Ag(110),[33] and recently for a large organic molecule on Cu(110).[24] Thermal activation is typical for adsorbate-induced reconstructions[34] and the common driving force with these systems is that the higher coordination of an adsorbate embedded in the surface layers leads to an overall increase in bonding energy. The associated energy barrier reflects the breaking of bonds in the surface necessary for vacancy formation. Similar phenomena have been reported on semiconductor surfaces: Yao *et al.* report a physisorbed C_{60} species on Si(100)(2×1) which becomes chemisorbed upon annealing and appears smaller in STM images.[19] They associate the transformation with the breaking of π bonds of Si dimers and the covalent bonding of C_{60} on top of them.

In conclusion we have presented the first detailed analysis of the bonding, mobility, and interactions of C_{60} at a metal surface at the single molecule level. The tracer diffusion of C_{60} adsorbed on the unreconstructed Pd(110) surface was analyzed and an energy barrier of (1.4 ± 0.2) eV for motions along $[1\bar{1}0]$ is determined. Upon annealing to $\approx$700 K the apparent height of C_{60} molecules in STM decreases substantially and their mobility is strongly reduced. This is ascribed to the release of substrate atoms resulting in higher C-Pd coordination for the stable C_{60} species accommodated in the formed microscopic pits. These findings demonstrate, in particular, that local reconstructions may account for the coexistence of distinct C_{60} species at surfaces.

*Email: johannes.barth@epfl.ch

[1] C. Joachim *et al.*, Nature (London) **408**, 541 (2000).
[2] H. Park *et al.*, Nature (London) **407**, 57 (2000).
[3] J. H. Schön *et al.*, Nature (London) **408**, 549 (2000).
[4] G. Gensterblum *et al.*, Phys. Rev. B **50**, 11 981 (1994).
[5] A. V. Hamza and M. Balooch, Chem. Phys. Lett. **201**, 404 (1993).
[6] P. A. Brühwiler *et al.*, Chem. Phys. Lett. **279**, 85 (1997).
[7] A. J. Maxwell *et al.*, Chem. Phys. Lett. **247**, 257 (1995).
[8] R. Fasel *et al.*, Phys. Rev. Lett. **76**, 4733 (1996).
[9] M. Ø. Pedersen *et al.*, Surf. Sci. **389**, 300 (1997).
[10] P. W. Murray *et al.*, Phys. Rev. B **55**, 9360 (1997).
[11] R. Fasel *et al.*, Phys. Rev. B **60**, 4517 (1999).
[12] M. T. Cuberes *et al.*, Appl. Phys. A: Mater. Sci. Process. **66**, 669 (1998).
[13] C. Cepek *et al.*, Phys. Rev. B **53**, 7466 (1996).
[14] M. Pedio *et al.*, Surf. Sci. **437**, 249 (1999).
[15] M. Pedio *et al.*, Phys. Rev. Lett. **85**, 1040 (2000).
[16] J. K. Gimzewski *et al.*, Phys. Rev. Lett. **72**, 1036 (1994).
[17] P. Rudolf, in *Proceedings of the International Winterschool on Electronic Properties of Novel Materials. Fullerenes and Fullerene Nanostructures* (World Scientific, Singapore, 1996), p. 263.
[18] A. V. Hamza, in *Fullerenes: Chemistry, Physics and Technology*, edited by K. M. Kadish and R. S. Ruoff (Wiley, New York, 2000), p. 531.
[19] X. Yao *et al.*, Appl. Phys. A: Mater. Sci. Process. **66**, 107 (1998).
[20] E. Giudice *et al.*, Surf. Sci. **405**, L561 (1998).
[21] C. Cepek *et al.*, Phys. Rev. B **63**, 125406 (2001).
[22] J. Weckesser *et al.*, J. Chem. Phys. **110**, 5351 (1999).
[23] J. V. Barth, Surf. Sci. Rep. **40**, 75 (2000).
[24] M. Schunack *et al.*, Phys. Rev. Lett. **86**, 456 (2001).
[25] J. Weckesser *et al.*, J. Chem. Phys. (to be published).
[26] J. V. Barth *et al.*, Phys. Rev. B **55**, 12 902 (1997).
[27] Y. Li *et al.*, Phys. Rev. B **56**, 12 539 (1997).
[28] L. H. Tjeng *et al.*, Solid State Commun. **103**, 31 (1997).
[29] J. Weckesser *et al.*, Surf. Sci. **431**, 268 (1999).
[30] W. Fan *et al.*, Phys. Rev. B **60**, 10 727 (1999).
[31] J. C. Hamilton *et al.*, Phys. Rev. B **61**, R5 425 (2000).
[32] R. Schuster *et al.*, Surf. Sci. **247**, L229 (1991).
[33] J. V. Barth *et al.* (unpublished).
[34] R. J. Behm *et al.*, in *Physics and Chemistry of Alkali Metal Adsorption*, edited by H. P. Bonzel, A. M. Bradshaw and G. Ertl (Elsevier, Amsterdam, 1989), p. 111.